Journal of Intelligent and Robotic Systems (2005) 42: 361–391

A Statistically-Switched Adaptive Vector Median Filter

RASTISLAV LUKAC*, KONSTANTINOS N. PLATANIOTIS and ANASTASIOS N. VENETSANOPOULOS
The Edward S. Rogers Sr. Department of ECE, University of Toronto, 10 King's College Road, Toronto, ON, M5S 3G4 Canada

BOGDAN SMOLKA
Department of Automatic Control, Silesian University of Technology, Akademicka 16 Str., 44-101 Gliwice, Poland

(Received: 29 April 2004; in final form: 29 October 2004)

Abstract. This paper presents a new cost-effective, adaptive multichannel filter taking advantage of switching schemes, robust order-statistic theory and approximation of the multivariate dispersion. Introducing the statistical control of the switching between the vector median and the identity operation, the developed filter enhances the detail-preserving capability of the standard vector median filter. The analysis and experimental results reported in this paper indicate that the proposed method is capable of detecting and removing impulsive noise in multichannel images. At the same time, the method is computationally efficient and provides excellent balance between the noise attenuation and signal-detail preservation. Excellent performance of the proposed method is tested using standard test color images as well as real images related to emerging virtual restoration of artworks.

Key words: nonlinear image processing, color image filtering, adaptive filter design, order-statistic theory, virtual restoration of artworks.

1. Introduction

Computer and machine vision methods find an application in novel commercial devices such as wireless phones, vision-based pocket devices, sensor networks, and surveillance and automotive apparatus [7, 10, 13]. Combining recent advances in the field of computer and machine vision, hardware, software, digital signal/image processing extends the possibilities of the traditional vision based communication between end-users or between machine and human.

Due to imperfections in image sensors, digital images are often contaminated with noise. Image imperfections resulting from impulsive noise are created during transmission through a communication channel, with sources ranging from human-made (switching and interference), to signal representation (bit errors), and natural (atmospheric lightning) [18]. The resulting noisy samples, so-called outliers, have

* Corresponding author e-mail: lukacr@dsp.utoronto.ca, Web: http//www.dsp.utoronto.ca/∼lukacr.

significantly deviating characteristics (e.g., amplitude in at least one of the components) compared to those of the neighboring samples. Noise affects the perceptual quality of the image, decreasing not only the appreciation of the image but also the performance of the task for which the image was intended. Therefore, image filtering used prior subsequent processing steps such as image analysis and compression is an essential part of any image processing system whether the final image is utilized for visual interpretation or for automatic analysis [26, 28].

Among the noise reduction techniques, vector processing techniques for multidimensional data set denoising take a great interest of image processing community. This can be attributed primarily to the importance of color image processing [18, 28]. The surge of emerging applications [18] such as web-based processing of color images and videos, enhancement of DNA microarray images, digital archiving and culture heritage preservation suggests that the demand for new, more powerful and cost-effective vector filtering solutions will continue.

The proposed here multichannel filtering scheme, viewed as the adaptive extension of the vector median filter [2] utilizes the statistical control of the smoothing levels and is appropriate for both image pre-processing and final restoration of noisy color image data. Moreover, it is computationally efficient and may decrease the average number of operations necessary in standard vector median filtering [2, 5] or switching vector filtering schemes recently introduced in [16]. The proposed cost-effective method removes unprofitable information in digital images without degradation of the underlying image structures and color information. Therefore, the method can be used not only in traditional color image applications, however, as it is demonstrated in this paper, it can be successfully used in virtual restoration of artworks.

The remainder of this paper is organized as follows. In the next section, the basic description of the vector median filter is presented. Section 3 focuses on the proposed method. Motivation and design characteristics of the proposed framework are discussed in detail. Section 4 introduces the analysis and properties of the proposed method. Section 5 is devoted to the experimental results. The computational complexity of the proposed method is analyzed in Section 6. Finally, conclusions are drawn in Section 7.

2. Vector Median Filter

In the last decade, a variety of filtering methods for multichannel image processing have been provided [2, 28, 31]. The common feature of vector filters relates to the consideration of the inherent correlation which exists between the image color channels. Since the vector approaches process an input signal as a set of vectors, color artifacts for which the human visual system is very sensitive [29] cannot be created as a filter output.

If the image information interferes with the impulsive noise or outliers (samples deviating from the data population), an efficient solution is provided by filters based

on robust order-statistics [3, 25, 26]. Since color images represent vector-valued image signals, the direct extension of order-statistic theory is impossible [24, 30] and thus, the observed samples are ordered according to specially developed distance functions.

Let $\mathbf{x}$: $Z^l \rightarrow Z^m$ represent a multichannel image, where l is an image dimension and m denotes the number of color channels. In the case of standard color images, parameters l and m are equal to 2 and 3, respectively. Let $W = \{\mathbf{x}_i \in Z^l;\ i = 1, 2, \ldots, N\}$ represent a filter window of a finite size N, where $\mathbf{x}_1, \mathbf{x}_2, \ldots, \mathbf{x}_N$ is a set of noisy samples and the central sample $\mathbf{x}_{(N+1)/2}$ determines the position of the filter window. Note that x_{ik}, for $k = 1, 2, \ldots, m$, is the kth element of the input sample $\mathbf{x}_i = (x_{i1}, x_{i2}, \ldots, x_{im})$.

Let us consider that each input multichannel sample $\mathbf{x}_i$ is associated with the distance measure

$$L_i = \sum_{j=1}^{N} \|\mathbf{x}_i - \mathbf{x}_j\|_2 \quad \text{for } i = 1, 2, \ldots, N, \tag{1}$$

where $\|\mathbf{x}_i - \mathbf{x}_j\|_2$ quantifies the distance among two m-channel samples $\mathbf{x}_i$ and $\mathbf{x}_j$ using the well-known Euclidean metric* given as [23, 28]:

$$\|\mathbf{x}_i - \mathbf{x}_j\|_2 = \left(\sum_{k=1}^{m} |x_{ik} - x_{jk}|^2 \right)^{1/2}, \tag{2}$$

where x_{ik} is the kth element of $\mathbf{x}_i$.

Assuming that the sums of the aggregated vector distances $L_1, L_2, \ldots, L_N$, which denote the sums of the aggregated vector distances, serve as the ordering criterion, i.e.

$$L_{(1)} \leqslant L_{(2)} \leqslant \cdots \leqslant L_{(N)} \tag{3}$$

and (3) implies the same ordering scheme to the input set $\mathbf{x}_1, \mathbf{x}_2, \ldots, \mathbf{x}_N$, the procedure results in the ordered sequence of color vectors written by

$$\mathbf{x}_{(1)} \leqslant \mathbf{x}_{(2)} \leqslant \cdots \leqslant \mathbf{x}_{(N)}. \tag{4}$$

Sample $\mathbf{x}_{(1)} \in W$ associated with the minimum vector distance $L_{(1)} \in \{L_1, L_2, \ldots, L_N\}$ constitutes the output of the vector median filter (VMF) [2] minimizing the distance to other samples inside the sliding filtering window W.

3. Proposed Adaptive Vector Median Filters

It is commonly observed that the standard low-pass filtering schemes operating on a fixed supporting window blur image details and eliminate fine image structures [17]. To avoid this drawback and preserve the structural content of the image,

* The Euclidean metric is the most popular member of the family generalized by the Minkowski metric [18, 23].

researchers try to extend the degree of freedom in designing color image filtering techniques, mostly through the introduction of the weighting coefficients. As a result, multichannel weighted filters can be adapted for various image and noise statistics [17, 19, 20, 27, 32]. If the environment is impulsive in the nature, the most popular and computationally efficient approaches are probably those related to the switching-based filtering [6, 8, 9, 14, 33]. In this case, the adaptive techniques alter the nonlinear mode (such as VMF) smoothing out noisy samples and the identity operation which remains the desired samples unchanged. It is not difficult to see that this filtering approach is useful in a wide range of applications, where outliers and noise impairments must be removed while the structural content and the color information should be preserved. Unfortunately, most of the switching-based filtering schemes have been developed for gray-scale imaging. The extension of these algorithms to color images may be problematic especially in terms of flexibility to accommodate the algorithm for a variety of window shapes [8, 33], computational complexity [33] or number of switching levels [9]. A multichannel switching scheme in [16] exhibits an excellent performance in color images corrupted by impulsive noise, however, these desired design characteristics are obtained at expense of the computational complexity. Therefore, an alternative solution is needed.

The proposed method is based on the robust order-statistics theory and approximation of the multivariate dispersion computed using the input multichannel samples. Its unique and distinguishing element is a statistical operator used to control the switching between the robust VMF and the identity operation. The input central sample is considered to be noisy if it lies outside the range formed by approximated multivariate dispersion of the input multichannel samples (Figure 1). To increase the degree of freedom in such a design, the proposed method:

(i) utilizes approximation of the multivariate dispersion multiplied by a certain regulation parameter,

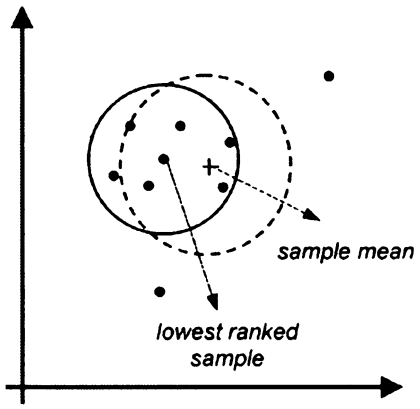

Figure 1. Modelling of the proposed concept in the 2-dimensional case. The vectors are classified using the variance multiplied by the adjusting parameter λ_1 or λ_2.

(ii) extends the concept of a gray-scale adaptive filtering scheme based on a weighted mean [14], and
(iii) determines the output using the most similar input vectors to the statistical centroid of the vectorial inputs.

Designing the proposed scheme, two ways are possible: radius of the spheres with centers in the lowest ranked vector and in the samples mean. To avoid the computational difficulties connected with calculation of variance–covariance matrices of multichannel samples [1, 21, 22], the proposed method utilizes approximation of the variance. In addition to this feature, the proposed framework is flexible and can be easily adapted for a large window size without any additional settings of the filter parameters.

3.1. FILTER DESIGN

Let ψ be the approximation of the multivariate variance of the vectors contained in a supporting window W of sufficiently large window size N, given by

$$\psi = \frac{L_{(1)}}{N-1}, \tag{5}$$

where $L_{(1)}$ is the distance measure calculated via (1) and (3). The quantity $L_{(1)}$ denotes the smallest aggregated distance associated with the VMF output $\mathbf{x}_{(1)}$, and can be expressed as follows:

$$L_{(1)} = \sum_{j=1}^{N} \|\mathbf{x}_{(1)} - \mathbf{x}_j\|_2. \tag{6}$$

This approximation defined in (5) represents the mean distance between the vector median and all other color pixels contained in W. The division of $L_{(1)}$ by $(N-1)$ denoting the number of distances from $\mathbf{x}_{(1)}$ to all samples from W ensures that the dispersion measure is non-dependent on the filtering window size.

Then, the output of the proposed adaptive vector median filter (AVMF) is defined as follows:

$$\mathbf{y}_{\text{AVMF}} = \begin{cases} \mathbf{x}_{(1)} & \text{for } L_{(N+1)/2} \geqslant \xi_1, \\ \mathbf{x}_{(N+1)/2} & \text{otherwise,} \end{cases} \tag{7}$$

where $\mathbf{y}_{\text{AVMF}}$ is the proposed AVMF output, $L_{(N+1)/2}$ obtained via (1) denotes the distance measure of the center pixel $\mathbf{x}_{(N+1)/2}$, the vector $\mathbf{x}_{(1)}$ is the VMF output obtained in (4) and ξ_1 is the threshold value given by

$$\xi_1 = L_{(1)} + \lambda_1 \psi = \frac{N-1+\lambda_1}{N-1} L_{(1)}, \tag{8}$$

where ψ is the approximated variance (5) and λ_1 is the tuning parameter used to adjust the smoothing properties of the proposed AVMF method.

If the distance measure $L_{(N+1)/2}$ of the central sample $\mathbf{x}_{(N+1)/2}$ is larger than the threshold ξ_1, then $\mathbf{x}_{(N+1)/2}$ is noisy and is being replaced with the lowest ranked vector $\mathbf{x}_{(1)}$. If the accumulated distance $L_{(N+1)/2}$ corresponding to the window center $\mathbf{x}_{(N+1)/2}$ is less or equal to ξ_1, then $\mathbf{x}_{(N+1)/2}$ is similar to most of the vectorial inputs and remains unchanged.

In order to follow both concepts shown in Figure 1, it is possible to modify the decision stage and replace the lowest ranked vector with the sample mean. Then approximation of the variance is given by

$$\psi_{\bar{\mathbf{x}}} = \frac{L_{\bar{\mathbf{x}}}}{N}, \tag{9}$$

where

$$L_{\bar{\mathbf{x}}} = \sum_{j=1}^{N} \|\bar{\mathbf{x}} - \mathbf{x}_j\|_2 \tag{10}$$

is the aggregated distance between multichannel input samples $\mathbf{x}_1, \mathbf{x}_2, \ldots, \mathbf{x}_N$ and the sample mean $\bar{\mathbf{x}}$.

In such a case, the output of the modified adaptive vector median filter (MAVMF) is defined as follows:

$$\mathbf{y}_{\text{MAVMF}} = \begin{cases} \mathbf{x}_{(1)} & \text{for } L_{(N+1)/2} \geqslant \xi_2, \\ \mathbf{x}_{(N+1/2)} & \text{otherwise,} \end{cases} \tag{11}$$

where ξ_2 is the threshold value defined by

$$\xi_2 = L_{\bar{\mathbf{x}}} + \lambda_2 \psi_{\bar{\mathbf{x}}} = \frac{N + \lambda_2}{N} L_{\bar{\mathbf{x}}} \tag{12}$$

and λ_2 is the adjusting parameter like in the AVMF scheme.

3.2. PROPOSED COLOR IMAGE PROCESSING PROCEDURE

Similarly to the conventional VMF operator, the proposed solutions use the local image statistics of the image vectors $\{\mathbf{x}_1, \mathbf{x}_2, \ldots, \mathbf{x}_N\}$ within a processing window W of finite size N. The window (Figure 2) slides over the entire image $\mathbf{x}$ placing successively every pixel at the center of a local neighborhood. The procedure replaces the sample $\mathbf{x}_{(N+1)/2}$ located at the window center with the output of a function (7) for the AVMF or (11) for the MAVF scheme, respectively, operating over the samples listed in W.

Note that the processing window may have various shapes which determine both the area of support and the overall performance of the processing procedure. The concept and the properties of the sliding (running) window are discussed in detail in [18]. Due to its versatility and demonstrated good performance the

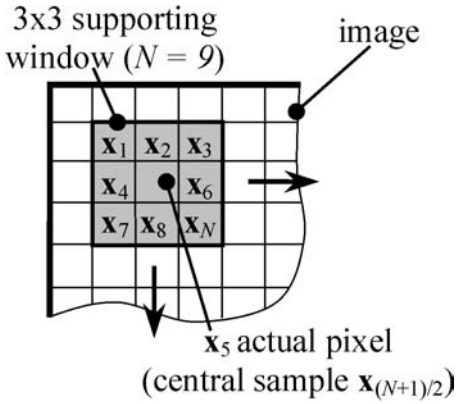

Figure 2. Arrangements of the vectorial inputs in the supporting window W sliding over the image domain.

3×3 rectangular shape window (Figure 2) is the most commonly used in image processing⋆ and the one to be used throughout the paper.

4. Filter Properties

The uniqueness of the proposed concept is demonstrated through the analysis of its most prominent properties. Although the properties listed in this section are derived mainly for the AVMF filter, many of them can be generalized also for the MAVMF scheme.

4.1. POSITIVITY OF THE ADJUSTING PARAMETER

Let us consider that $\mathbf{x}_{(1)} \in \{\mathbf{x}_1, \mathbf{x}_2, \ldots, \mathbf{x}_N\}$ is the lowest ranked vector, i.e. the sample associated with the smallest aggregated distance $L_{(1)} \in \{L_1, L_2, \ldots, L_N\}$. Because $\mathbf{x}_{(1)}$ minimizes the distance to other samples inside W, and thus $L_{(N+1)/2} \geqslant L_{(1)}$, their relationship is given by

$$L_{(N+1)/2} = L_{(1)} + \Delta. \tag{13}$$

Then, considering the switching rule used in (7) it results in the following inequality

$$\frac{\Delta}{L_{(1)}} \geqslant \frac{\lambda_1}{N-1}. \tag{14}$$

⋆ The processing filters operating on the larger area of support such as those determined by a 5×5 or 7×7 window may have better noise attenuation capability than the employed here 3×3 filters. However, this improvement is accompanied by the substantial degradation of the essential filters' preserving characteristics and at the same time, the use of the larger window significantly increases computational expenses.

This expression shows that the adjusting parameter λ_1 has to be a nonnegative number, because the right side of (14) is always nonnegative.

4.2. BOUNDARY OF THE IDENTITY OPERATION

Depending on condition (14) it is clear that the proposed method will perform the identity operation for any value of λ_1, if and only if the lowest ranked vector $\mathbf{x}_{(1)}$ is identical with the central sample $\mathbf{x}_{(N+1)/2}$ and thus $\Delta = 0$. This property is interesting in the context of deterministic properties usually expressed through the analysis of root signals. Assuming that $\mathbf{x}_{(1)} \neq \mathbf{x}_{(N+1)/2}$ the AVMF output is a root if and only if the ratio $\Delta / L_{(1)}$ is larger than or equal to the tuning element $\lambda_1/(N-1)$. Note that the second extreme for the identity operation can be expressed by

$$(N-2)(N-1) \geqslant \lambda_1 \tag{15}$$

which means that an additional increasing of λ_1, e.g., up 56 in the case of a 3×3 filtering window, makes the filter idempotent.

4.3. CONVERGENCE TO VMF AND IDENTITY OPERATION

The filtering efficiency depends on the adjusting parameter λ_1. If $\lambda_1 = 0$, then the filter output is always the VMF. On the other hand, for big values of λ_1 the proposed filter output will be always the central pixel $\mathbf{x}_{(N+1)/2}$ as follows:

$$\mathbf{y} = \begin{cases} \mathbf{x}_{(1)} & \text{if } \lambda_1 = 0, \\ \mathbf{x}_{(N+1)/2} & \text{if } \lambda_1 \to \infty. \end{cases} \tag{16}$$

4.4. CAPABILITY OF LOW-PASS FILTERING

The previous property determines the range of output samples. Since the output of the proposed AVMF and MAVMF filters is always restricted to be the input central sample $\mathbf{x}_{(N+1)/2}$ or the lowest ranked vector $\mathbf{x}_{(1)}$ and both samples belong to the input set W, the output of the proposed method can never be outside the range of input samples inside W. It means that the proposed method is only capable of low-pass filtering.

4.5. SCALE AND BIAS NON-DEPENDENCE

Let us consider the input set $W_1 = \{\mathbf{x}_i^1 \in Z^l;\ i = 1, 2, \ldots, N\}$ and the modified input set $W_2 = \{\mathbf{x}_i^2 \in Z^l;\ i = 1, 2, \ldots, N\}$ achieved by adding the vector constant $\mathbf{k}$ to the input set W_1 multiplied by scalar constant k, i.e. $\mathbf{x}_i^2 = k\mathbf{x}_i^1 + \mathbf{k}$. It can be easily shown that adding the vector constant has no influence on a filter control, since vector distances $L_1(W_1), L_2(W_1), \ldots, L_N(W_1)$ are equivalent to $L_1(W_2), L_2(W_2), \ldots, L_N(W_2)$. The multiplied input set has also no influence on the switching condition $L_{(N+1)/2} \geqslant ((N-1+\lambda_1)/(N-1))L_{(1)}$, since

$$L_{(N+1)/2}(W_2) = kL_{(N+1)/2}(W_1), \tag{17}$$

$$L_{(1)}(W_2) = kL_{(1)}(W_1), \tag{18}$$

and then

$$L_{(N+1)/2}(W_1) \geqslant \frac{N-1+\lambda_1}{N-1} L_{(1)}(W_1), \tag{19}$$

$$L_{(N+1)/2}(W_2) \geqslant \frac{N-1+\lambda_1}{N-1} L_{(1)}(W_2) \tag{20}$$

are equivalent.

Thus, the decision stage of the proposed method is scale and bias non-dependent.

4.6. EQUIVALENCE BETWEEN AVMF AND MAVMF

Both proposed methods are equivalent, if a special relation between ξ_1 and ξ_2 is satisfied. Let us consider λ_1 and λ_2 as adjusting parameters in the AVMF and MAVMF schemes, respectively, and the threshold values ξ_1 and ξ_2 defined by (8) and (12). Then, both filters are equivalent if and only if $\xi_1 = \xi_2$ and thus

$$\frac{L_{(1)}}{L_{\bar{\mathbf{x}}}} = \frac{(N-1)(N+\lambda_2)}{N(N-1+\lambda_1)}. \tag{21}$$

From (21) it is clear that for $\lambda_1 = 0$ and $\lambda_2 = 0$, both filters are equivalent if and only if $L_{(1)} = L_{\bar{\mathbf{x}}}$. Note that this equivalence can occur only in monotonous noise-free image area, when the VMF and the sample mean are equivalent.

5. Experimental Results

Performance of the proposed multichannel filtering tools is evaluated in the most important area of vector processing, namely color image filtering.* Note that all filtering results presented in this paper were obtained with a 3×3 square window, i.e. for $N = 9$. In order to compare the performance of the new method with the state-of-the-art color image filters, we used the standard test images shown in Figures 3(a)–(c), their corrupted versions depicted in Figures 3(d)–(f) and also real images shown in Figures 12(a), (d).

5.1. RESULTS ACHIEVED USING STANDARD TEST IMAGES

The 256×256 color test images shown in Figures 3(a)–(c) have been contaminated by impulsive noise (Figures 3(d)–(f)) defined as follows [17]:

$$\mathbf{x}_i = \begin{cases} \mathbf{v}_i & \text{with probability } p_{\mathbf{v}}, \\ \mathbf{o}_i & \text{with probability } 1 - p_{\mathbf{v}}, \end{cases} \tag{22}$$

* The figures in this paper can be seen in color at http://www.dsp.utoronto.ca/~lukacr/color4.pdf.

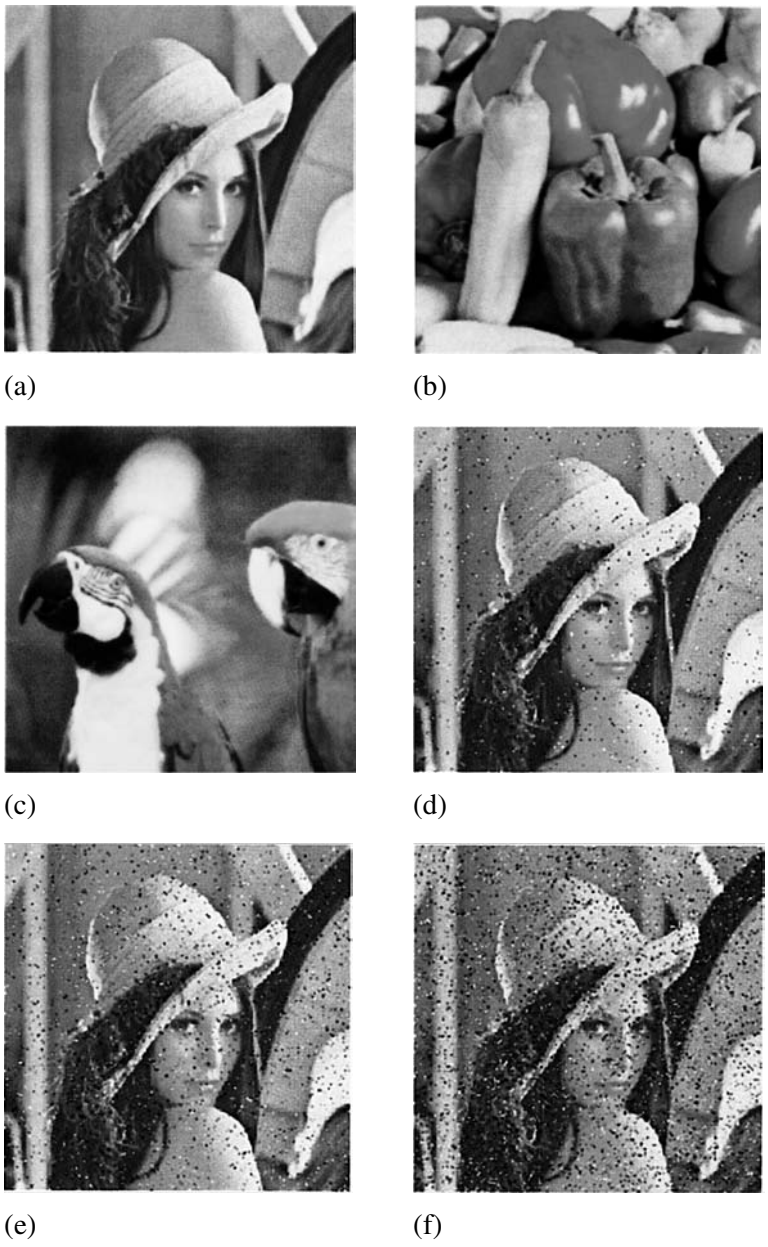

Figure 3. Test images: (a) original image Lena, (b) original image Peppers, (c) original image Parrots, (d)–(f) image Lena corrupted by impulsive noise with the probability: (d) $p_{\mathbf{v}} = 0.05$, (e) $p_{\mathbf{v}} = 0.10$ and (f) $p_{\mathbf{v}} = 0.20$.

where i characterizes the sample position, $\mathbf{o}_i$ is the original sample, $\mathbf{x}_i$ represents the sample from the noisy image and $p_{\mathbf{v}}$ is a corruption probability (also termed the percentage number of corrupted pixels). The impulse $\mathbf{v}_i = (v_{i1}, v_{i2}, \ldots, v_{im})$ is in-

dependent from pixel to pixel and has generally much larger and smaller amplitude than the neighboring samples at least in one of the components.

The accuracy of the proposed switching mechanisms is evaluated using the impulse successful detection (SDT) and false detection (FDT) criteria. The SDT and FDT rates are obtained as follows [16]:

$$\text{SDT} = \frac{\eta - \varepsilon_c}{\eta} \cdot 100, \tag{23}$$

$$\text{FDT} = \frac{\varepsilon_m}{K_1 K_2 - \eta} \cdot 100, \tag{24}$$

where ε_m denotes the number of noise-free samples detected as impulses, ε_c is the number of undetected impulses, η denotes the total number of impulses and the product $K_1 K_2$ is the number of image samples.

To provide some measure of closeness between two digital images, a number of different objective measures based on the difference in the statistical distributions of the pixel values can be utilized. In this paper, we will make use of the commonly employed objective measures [19] such as the mean absolute error (MAE), the mean square error (MSE) and the normalized color difference (NCD) criterion. The MAE and MSE are defined as follows:

$$\text{MAE} = \frac{1}{m K_1 K_2} \sum_{k=1}^{m} \sum_{i=1}^{K_1 K_2} |o_{ik} - x_{ik}|, \tag{25}$$

$$\text{MSE} = \frac{1}{m K_1 K_2} \sum_{k=1}^{m} \sum_{i=1}^{K_1 K_2} (o_{ik} - x_{ik})^2, \tag{26}$$

where $\mathbf{o}_i = (o_{i1}, o_{i2}, \ldots, o_{im})$ is the original pixel, $\mathbf{x}_i = (x_{i1}, x_{i2}, \ldots, x_{im})$ is the noisy (or restored) pixel, i is the pixel position in a $K_1 \times K_2$ color image and k characterizes the color channel.

The measure of color distortion is, in the perceptual way to humans, evaluated using the NCD criterion defined as follows [27, 28]:

$$\text{NCD} = \frac{\sum_{i=1}^{K_1 K_2} \sqrt{(L^*_{\mathbf{o}_i} - L^*_{\mathbf{x}_i})^2 + (u^*_{\mathbf{o}_i} - u^*_{\mathbf{x}_i})^2 + (v^*_{\mathbf{o}_i} - v^*_{\mathbf{x}_i})^2}}{\sum_{i=1}^{K_1 K_2} \sqrt{(L^*_{\mathbf{o}_i})^2 + (u^*_{\mathbf{o}_i})^2 + (v^*_{\mathbf{o}_i})^2}}, \tag{27}$$

where L^* represents lightness values and (u^*, v^*) chrominance values corresponding to original $\mathbf{o}_i$ and noisy (or filtered) $\mathbf{x}_i$ samples expressed in CIELUV color space [29].

The comparison of the structure of both proposed methods suggests that the suboptimal value of λ_2 used in the MAVMF scheme should be larger than that λ_1 of the AVMF approach. Visual inspection of the results depicted in Figures 4–6 reveals that the optimal value of λ_1 and λ_2 slightly decreases with the degree of the noise corruption. It also confirms that the MAVMF scheme should correspond

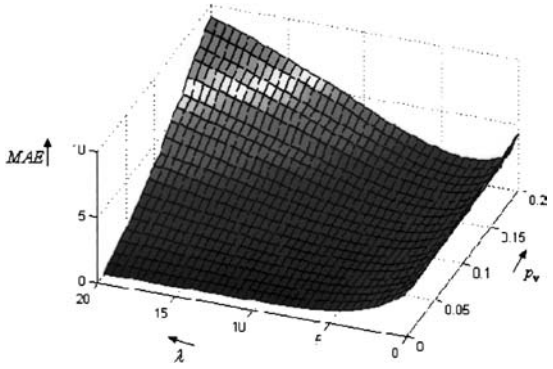

(a)

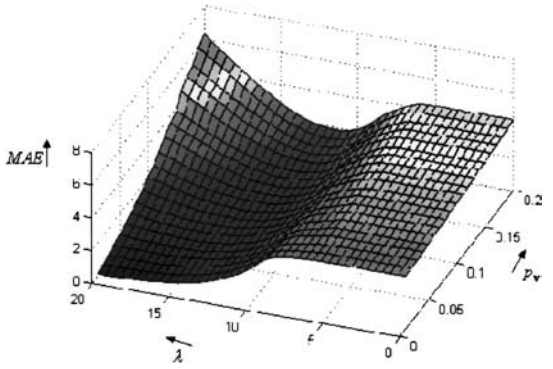

(b)

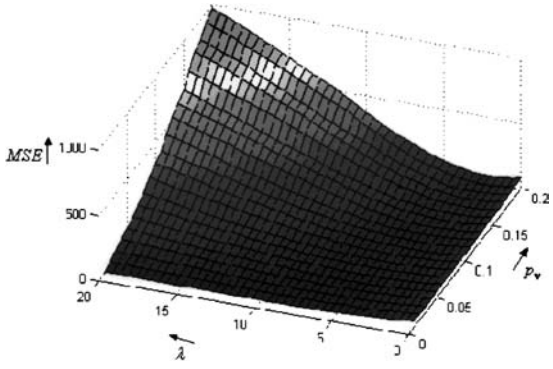

(c)

Figure 4. Performance of AVMF and MAVMF techniques in dependence on adjusting parameters λ_1, λ_2 and impulsive noise intensity $p_{\mathbf{v}}$ using the test image Lena; (a), (c), (e) AVMF, (b), (d), (f) MAVMF.

to larger value of λ_2 in comparison with λ_1 of the AVMF. Note that these results were achieved using the test image Lena (Figure 3(a)), Peppers (Figure 3(b)) and

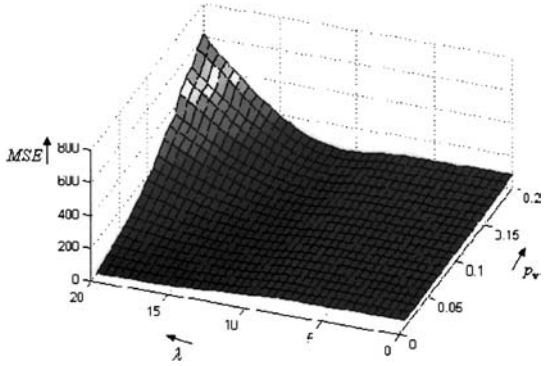

(d)

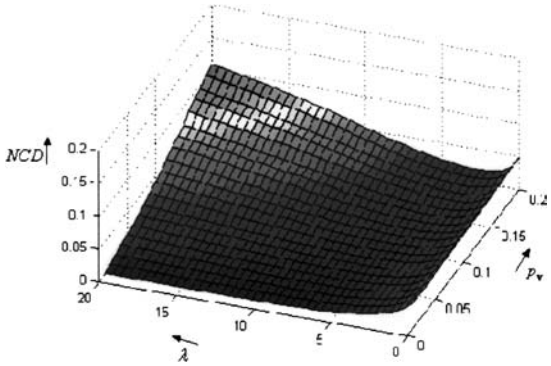

(e)

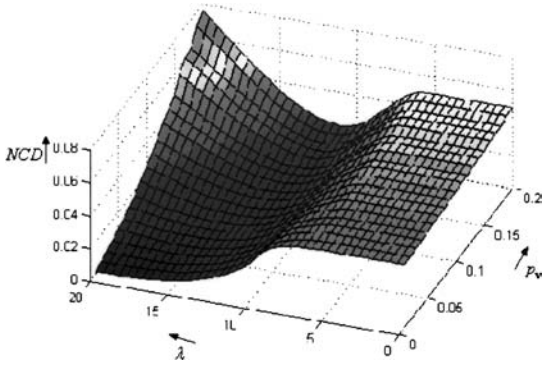

(f)

Figure 4. (Continued.)

Parrots (Figure 3(c)) corrupted by impulsive noise with intensity $p_{\mathbf{v}}$ ranged from $p_{\mathbf{v}} = 0.01$ (1% noise) to $p_{\mathbf{v}} = 0.20$ (20% noise) with stepsize 0.01. The results presented in the sequence were obtained using $\lambda_1 = 4$ and $\lambda_2 = 12$ denoting the robust settings of the adjusting parameter used in the proposed schemes.

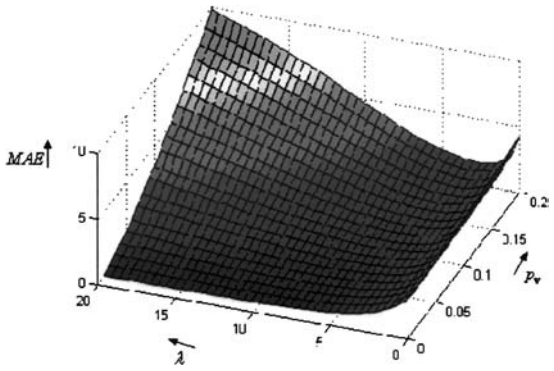

(a)

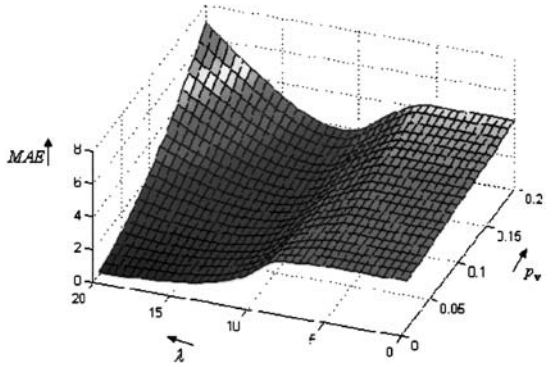

(b)

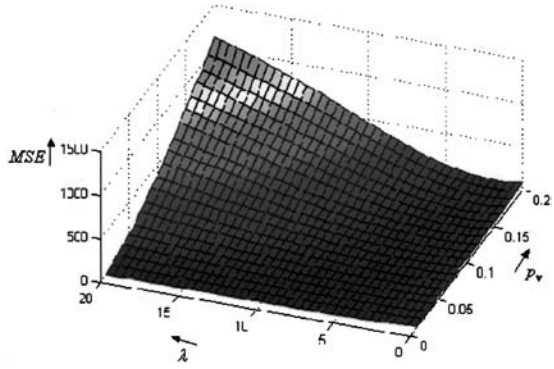

(c)

Figure 5. Performance of AVMF and MAVMF techniques in dependence on adjusting parameters λ_1, λ_2 and impulsive noise intensity p_v using the test image Peppers; (a), (c), (e) AVMF, (b), (d), (f) MAVMF.

Tables I–IV summarize the detection rates observed for the switching schemes such as the adaptive componentwise switching medians based on local contrast

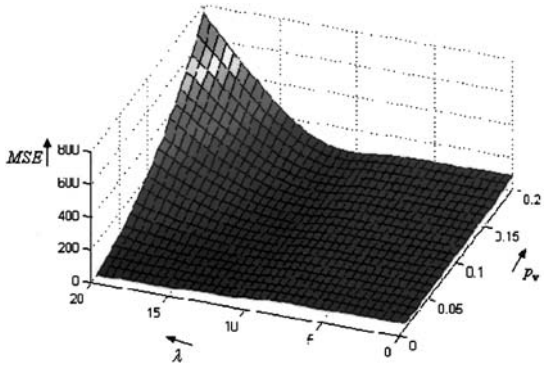

(d)

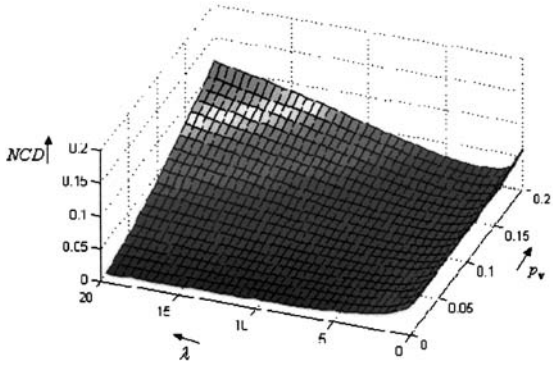

(e)

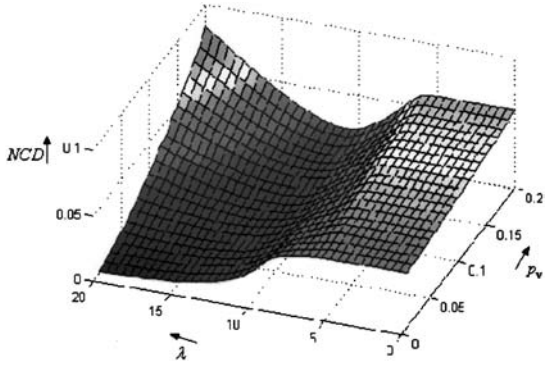

(f)

Figure 5. (Continued.)

probability (LCP) [6] and the standard deviation of the input set (SF) [14]. The representatives of the vector switching schemes include the switching center-weighted vector directional filter (SCWVDF) [16] and the proposed AVMF and MAVMF

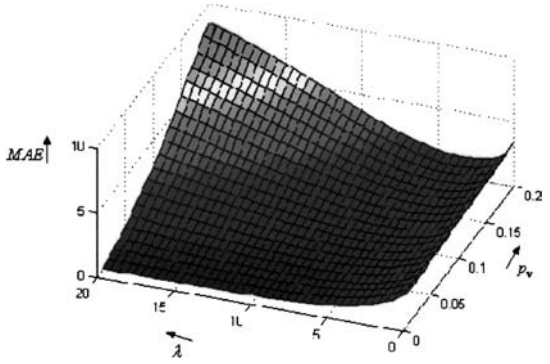

(a)

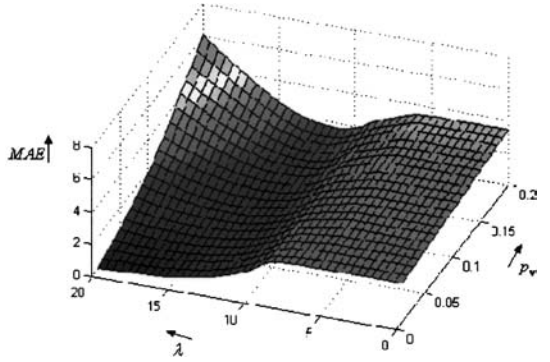

(b)

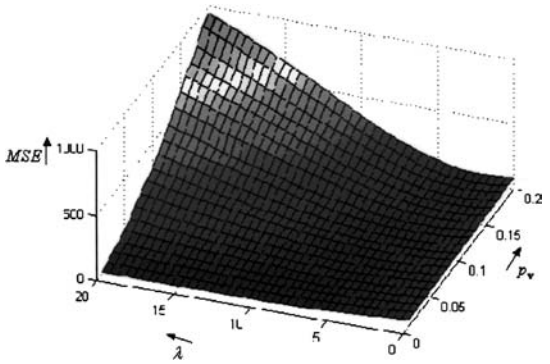

(c)

Figure 6. Performance of AVMF and MAVMF techniques in dependence on adjusting parameters λ_1, λ_2 and impulsive noise intensity p_v using the test image Parrots; (a), (c), (e) AVMF, (b), (d), (f) MAVMF.

solutions. The reported results indicate that the proposed schemes achieve an excellent trade-off between the SDT and FDT rates and hold these characteristics for the entire range of considered p_v. Note that the use of detection rates does

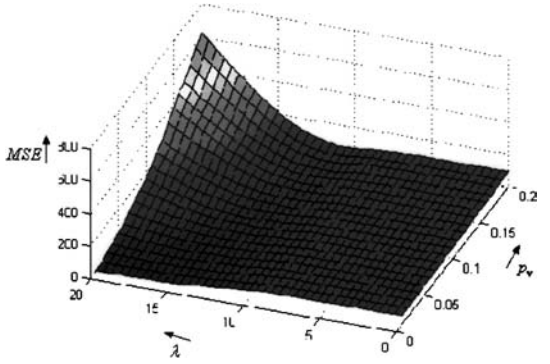

(d)

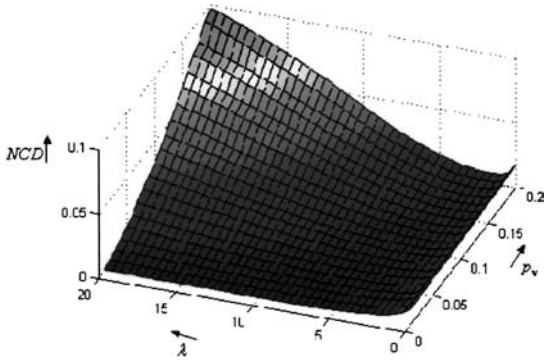

(e)

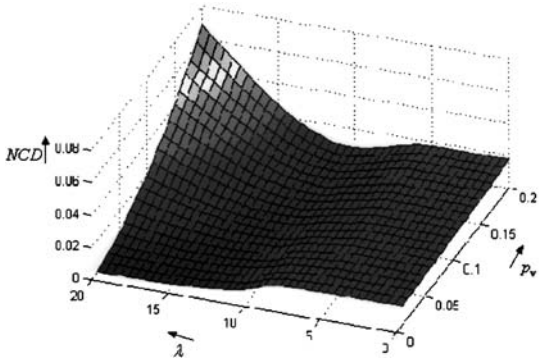

(f)

Figure 6. (Continued.)

not express the quality of the output image which is influenced by accuracy of both the switching mechanism and the smoothing filter. Therefore, the use of the conventional image quality measures (25)–(27) has a greater information value.

Table I. Comparison of the detection capability using impulsive noise corruption $p_{\mathbf{v}} = 0.05$.

Image	Lena		Peppers		Parrots	
Method	FDT	SDT	FDT	SDT	FDT	SDT
LCP	39.084	99.758	37.923	99.433	30.686	99.636
SF	27.929	99.073	27.139	98.784	22.209	90.190
SCWVDF	0.358	97.736	0.799	96.919	0.125	96.996
Proposed AVMF	7.042	98.563	6.931	97.430	5.556	98.518
Proposed MAVMF	10.255	98.845	10.439	97.946	9.286	98.353

Table II. Comparison of the detection capability using impulsive noise corruption $p_{\mathbf{v}} = 0.10$.

Image	Lena		Peppers		Parrots	
Method	FDT	SDT	FDT	SDT	FDT	SDT
LCP	31.123	99.415	29.957	99.051	23.042	99.130
SF	20.836	98.579	20.204	98.166	15.844	98.239
SCWVDF	0.360	96.631	0.828	95.840	0.144	96.519
Proposed AVMF	5.042	97.266	5.193	97.094	4.248	97.904
Proposed MAVMF	7.286	97.527	7.706	96.803	6.947	97.995

Table III. Comparison of the detection capability using impulsive noise corruption $p_{\mathbf{v}} = 0.20$.

Image	Lena		Peppers		Parrots	
Method	FDT	SDT	FDT	SDT	FDT	SDT
LCP	20.963	98.580	20.884	98.173	14.361	98.341
SF	12.247	96.668	11.944	96.554	8.917	96.604
SCWVDF	0.405	94.850	1.112	93.644	0.134	95.211
Proposed AVMF	2.539	95.296	2.217	95.375	2.014	95.451
Proposed MAVMF	5.060	95.338	5.376	95.824	4.350	95.533

Table IV. Comparison of the detection capability using impulsive noise corruption $p_{\mathbf{v}} = 0.30$.

Image	Lena		Peppers		Parrots	
Method	FDT	SDT	FDT	SDT	FDT	SDT
LCP	16.315	97.638	16.061	97.075	11.338	96.933
SF	8.196	95.130	8.286	94.402	6.318	94.688
SCWVDF	0.913	87.602	1.902	86.433	0.783	88.639
Proposed AVMF	1.270	89.362	1.357	88.508	1.227	90.476
Proposed MAVMF	1.995	88.140	1.987	87.405	1.836	89.116

Tables V–VIII summarize the objective results obtained using the MAE, MSE and NCD error criteria. The results correspond to the use of the test images shown in Figures 3(a)–(c). The proposed methods are compared with the componentwise median filter (MF) [34], the adaptive componentwise LCP and SF techniques, and the vector filtering schemes such as the VMF, the basic vector directional filter (BVDF) [31], the directional distance filter (DDF) [12], the generalized vector directional filter (GVDF) [31], the spherical median (SMF) [31], the hybrid vector filters (HVF_1, HVF_2) [11], and the SCWVDF [16]. The obtained results indicate that the proposed filters are clearly superior and outperform other (standard and adaptive) filtering techniques including the CWVDF scheme in terms of the robustness expressed through all objective image quality measures. For the images corrupted by impulsive noise with the noise intensity $p_{\mathbf{v}} > 0.30$, re-optimization of the filter parameter may be recommended to obtain the robust smoothing capability. It should be emphasized that the switching schemes such as the considered AVMF and MAVMF are primarily geared to address to the problem of impulsive noise removal in the images with a low or moderate amount of corrupted pixels. For such a task, the proposed solutions hold excellent performance.

Figures 7–10 allow for the visual comparison of the images recorded at the various stages of a processing pipeline. Visual inspection of the images depicted in Figures 7 and 9 reveal that the detail-preserving capability of the proposed method is satisfactory. Figures 8 and 10 depict the enlarged parts of the original, noisy and

Table V. Comparison of the presented filters using impulsive noise corruption $p_{\mathbf{v}} = 0.05$.

Image	Lena			Peppers			Parrots		
Method/ Criterion	MAE	MSE	NCD	MAE	MSE	NCD	MAE	MSE	NCD
Noisy	3.762	427.3	0.0445	3.988	486.1	0.0441	3.805	443.6	0.0432
MF	3.394	49.7	0.0442	3.248	43.1	0.0484	2.718	63.1	0.0170
VMF	3.430	50.8	0.0403	3.169	43.9	0.0452	2.669	64.2	0.0132
BVDF	3.818	58.6	0.0407	3.740	60.7	0.0438	3.460	109.0	0.0116
DDF	3.509	52.3	0.0402	3.182	44.6	0.0431	2.645	65.3	0.0117
GVDF	3.587	55.3	0.0420	3.433	57.9	0.0453	3.036	93.6	0.0126
SMF	3.523	45.6	0.0406	3.442	42.9	0.0456	2.927	61.6	0.0130
HVF_1	3.587	51.8	0.0410	3.282	42.9	0.0441	2.786	65.7	0.0122
HVF_2	3.573	50.4	0.0409	3.274	41.9	0.0441	2.771	63.5	0.0121
SF	1.764	33.3	0.0204	1.614	27.7	0.0217	1.416	45.5	0.0067
LCP	2.214	38.8	0.0263	2.046	33.1	0.0279	1.747	51.4	0.0086
SCWVDF	0.419	13.4	0.0040	0.538	18.0	0.0070	0.405	20.5	0.0013
AVMF	0.777	18.3	0.0082	0.729	16.5	0.0090	0.699	27.8	0.0027
MAVMF	0.980	21.4	0.0103	0.878	18.2	0.0107	0.840	31.1	0.0031

Table VI. Comparison of the presented algorithms using impulsive noise corruption $p_{\mathbf{v}} = 0.10$.

Image	Lena			Peppers			Parrots		
Method/ Criterion	MAE	MSE	NCD	MAE	MSE	NCD	MAE	MSE	NCD
Noisy	7.312	832.0	0.0840	7.677	943.3	0.0869	7.526	882.0	0.0857
MF	3.703	56.8	0.0489	3.579	53.9	0.0546	2.960	70.0	0.0198
VMF	3.687	56.5	0.0428	3.503	55.0	0.0494	2.890	69.6	0.0142
BVDF	4.099	67.6	0.0432	4.151	82.7	0.0484	3.630	113.5	0.0127
DDF	3.733	57.3	0.0424	3.512	56.6	0.0475	2.839	69.7	0.0128
GVDF	3.925	66.8	0.0448	3.785	73.4	0.0492	3.188	96.2	0.0137
SMF	3.907	53.1	0.0439	3.723	52.3	0.0499	3.133	67.1	0.0141
HVF_1	3.857	56.9	0.0434	3.626	53.6	0.0485	3.002	69.9	0.0132
HVF_2	3.840	55.5	0.0433	3.614	52.4	0.0485	2.999	68.6	0.0131
SF	1.775	37.1	0.0207	1.667	36.2	0.0225	1.507	51.6	0.0078
LCP	2.254	43.1	0.0271	2.101	41.6	0.0288	1.824	57.3	0.0095
SCWVDF	0.800	26.7	0.0072	0.979	41.8	0.0113	0.754	38.6	0.0025
AVMF	0.959	25.9	0.0105	0.941	27.4	0.0117	0.862	35.4	0.0041
MAVMF	1.123	28.3	0.0121	1.063	29.0	0.0133	1.016	40.6	0.0047

Table VII. Comparison of the presented algorithms using impulsive noise corruption $p_{\mathbf{v}} = 0.20$.

Image	Lena			Peppers			Parrots		
Method/ Criterion	MAE	MSE	NCD	MAE	MSE	NCD	MAE	MSE	NCD
Noisy	14.019	1604.6	0.1625	14.912	1832.0	0.1694	14.213	1663.0	0.1608
MF	4.521	87.9	0.0619	4.487	91.4	0.0726	3.623	97.3	0.0276
VMF	4.335	80.3	0.0492	4.232	85.7	0.0601	3.448	91.9	0.0174
BVDF	4.859	107.8	0.0499	5.111	152.9	0.0602	4.183	140.0	0.0165
DDF	4.321	78.8	0.0483	4.254	90.4	0.0579	3.386	91.2	0.0161
GVDF	4.345	83.4	0.0493	4.562	122.4	0.0586	3.450	100.9	0.0174
SMF	4.617	74.9	0.0505	4.554	82.3	0.0620	3.749	97.8	0.0181
HVF_1	4.548	80.4	0.0500	4.411	86.4	0.0599	3.594	92.7	0.0169
HVF_2	4.547	79.5	0.0499	4.409	84.5	0.0599	3.599	91.5	0.0168
SF	2.295	66.5	0.0284	2.267	73.6	0.0326	2.036	83.4	0.0136
LCP	2.739	70.6	0.0345	2.743	79.5	0.0404	2.290	85.0	0.0148
SCWVDF	1.826	84.2	0.0163	2.269	124.3	0.0244	1.626	90.8	0.0067
AVMF	1.816	77.6	0.0212	1.898	97.3	0.0251	1.618	90.0	0.0116
MAVMF	1.928	75.4	0.0221	1.995	94.2	0.0266	1.803	96.3	0.0128

Table VIII. Comparison of the presented algorithms using impulsive noise corruption $p_{\mathbf{v}} = 0.30$.

Image	Lena			Peppers			Parrots		
Method/ Criterion	MAE	MSE	NCD	MAE	MSE	NCD	MAE	MSE	NCD
Noisy	20.111	2313.1	0.2312	21.052	2567.2	0.2383	20.223	2368.8	0.2275
MF	5.576	140.2	0.0774	5.659	156.1	0.0954	4.585	146.7	0.0389
VMF	5.049	115.8	0.0557	5.104	137.0	0.0723	4.132	125.6	0.0215
BVDF	5.903	185.7	0.0576	6.743	304.6	0.0768	4.851	190.7	0.0212
DDF	5.002	114.2	0.0545	5.178	146.2	0.0707	3.991	120.8	0.0199
GVDF	4.758	110.5	0.0533	5.050	155.8	0.0658	3.701	112.7	0.0202
SMF	4.921	106.9	0.0548	5.017	125.3	0.0680	3.895	108.4	0.0215
HVF_1	5.383	117.4	0.0577	5.492	145.9	0.0761	4.351	128.9	0.0215
HVF_2	5.391	115.4	0.0576	5.485	141.9	0.0761	4.375	126.8	0.0215
SF	3.161	110.3	0.0418	3.417	139.2	0.0536	3.024	138.6	0.0237
LCP	3.727	126.0	0.0481	3.839	149.7	0.0616	3.240	142.8	0.0254
SCWVDF	3.279	194.3	0.0279	4.217	321.1	0.0443	2.944	203.1	0.0136
AVMF	2.803	132.9	0.0310	3.030	169.9	0.0402	2.548	144.7	0.0184
MAVMF	2.676	100.4	0.0287	2.882	130.4	0.0390	2.516	120.4	0.0157

(a) (b)

Figure 7. Results obtained by filtering the image shown in Figure 3(e): (a) VMF output, (b) proposed AVMF output.

output (filtered) images. Figures 8(c) and 10(c) show that the VMF scheme excellently suppresses impulses present in the image, however some edges and image details are heavily blurred, especially at transitions between image regions. As it can be seen in Figures 8(d) and 10(d) the use of the proposed adaptive principle improves signal-detail preserving capability of the VMF.

Figure 11 demonstrates robustness of the selected schemes. The proposed methods are compared against the filtering schemes such as MF, VMF, BVDF and LCP.

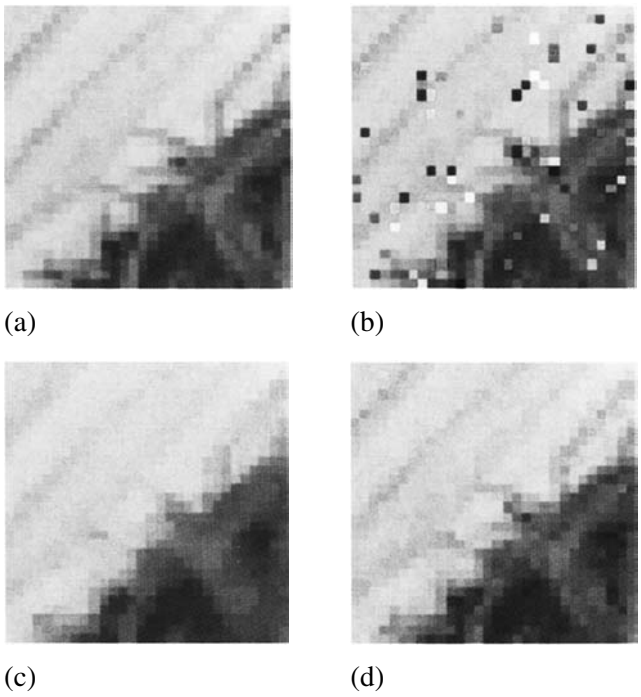

Figure 8. Zoomed parts of test images and achieved results related to the test image Lena: (a) original image Lena, (b) test image Lena corrupted by impulsive noise $p_{\mathbf{v}} = 0.10$, (c) VMF, (d) proposed AVMF.

Note that the degree of impulsive noise corruption $p_{\mathbf{v}}$ ranged from no corruption ($p_{\mathbf{v}} = 0$) to 20% impulsive noise ($p_{\mathbf{v}} = 0.20$) with the stepsize $p_{\mathbf{v}} = 0.01$. It can be seen that the proposed method achieves the best trade-off among objective criteria (MAE, MSE and NCD). Moreover, the proposed schemes hold excellent performance for a wide range of impulsive noise corruption $p_{\mathbf{v}}$. These results demonstrate the unique capability of the proposed method to remove image noise and simultaneously preserve color information and structural content of the image.

5.2. APPLICATION OF THE PROPOSED METHOD IN VIRTUAL RESTORATION OF ARTWORKS

Supported by the growth of multimedia technology and by the availability of effective electronic imaging tools, image-processing techniques have recently been applied to the analysis, preservation, and restoration of artworks [4, 15, 35]. Color image techniques can be used as a guide to the actual restoration of the artwork (computer-guided restoration). Or, they can produce a digitally restored version of the work, which itself is valuable although the restoration is only virtual and cannot be reproduced on the real piece of work (virtual restoration). In the case of virtual

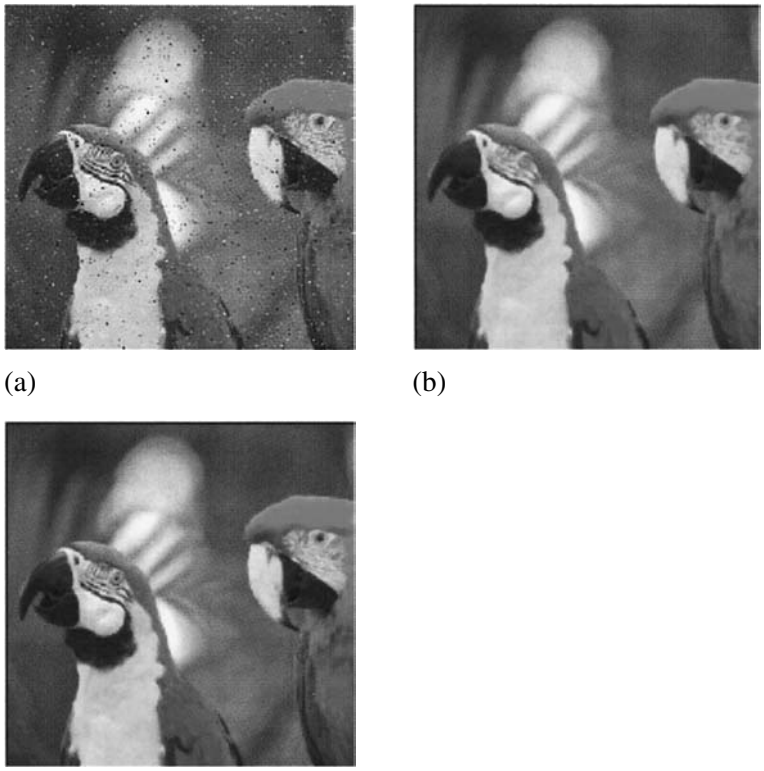

Figure 9. Results corresponding to Figure 3(c): (a) noisy image with $p_{\mathbf{v}} = 0.05$, (b) VMF output, (c) proposed AVMF output.

restoration and digital artwork libraries, the digital processing systems are designed to remove cracks and granulation artifacts (outliers in nature) from the artworks such as old paintings, frescos and roll documents. These artifacts decrease the effect of digital visualization Figures 12(a), (d) because they severely deteriorate the aspect of paintings and thus, the color digital restoration, color filtering and color image enhancement techniques are of key importance and, even if the removal is only virtual. Thus, the quality of the virtual restoration depends on some factors such as determining the original pigment and true color information.

Visual inspection of the results depicted in Figures 12 and 13 suggests that the adaptive vector techniques providing excellent trade-off between the noise attenuation and signal-detail preserving characteristics have a great potential to be used in virtual restoration of artworks. As it is shown in Figures 13(b), (e), the excessive smoothing capability of the VMF scheme results in blurred edges and fine details. However, the use of the proposed method preserves textures excellently while still exhibiting the sufficient noise attenuation capability Figures 13(c), (f).

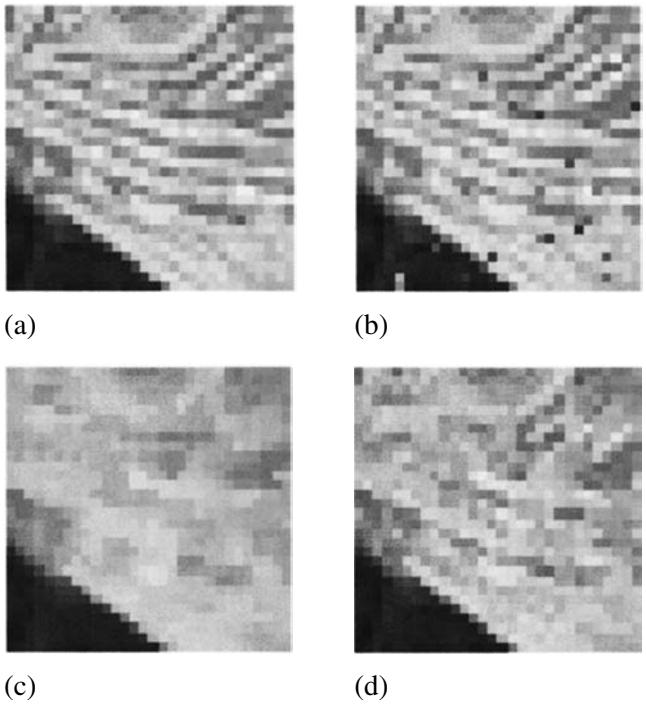

Figure 10. Zoomed parts of test images and achieved results related to the test image Parrots: (a) original image Parrots, (b) test image Parrots corrupted by impulsive noise $p_{\mathbf{v}} = 0.05$, (c) VMF, (d) proposed AVMF.

6. Computational Complexity Analysis

Apart from the numerical behavior (actual performance) of any algorithm, its computational complexity is a realistic measure of its practicality and usefulness. Therefore, the most special vector processing solutions are analyzed here in terms of normalized operations, such as additions (ADDs), multiplications (MULTs), divisions (DIVs), square roots (SQRTs), comparisons (COMPs) and arc cosines (ARCCOSs).

Table IX summarizes the total number of operations for the well-known vector processing solutions (VMF, BVDF, DDF), the SCWVDF scheme and the proposed adaptive filters (AVMF, MAVMF). The proposed adaptive vector filters are computationally efficient, since they perform practically the same set of operations as their non-adaptive special case VMF [2, 5]. The implementation of the AVMF and the VMF techniques shows that both schemes need to compute the aggregated distances and search for the minimum of them. The switching rule in the AVMF scheme requires an extra addition, multiplication, division and comparison operation. If the MAVMF scheme is used to process the images, the computational complexity is further decreased. In the case of noise-free samples the MAVMF filter performs the identity operation and excludes the time consuming calculations

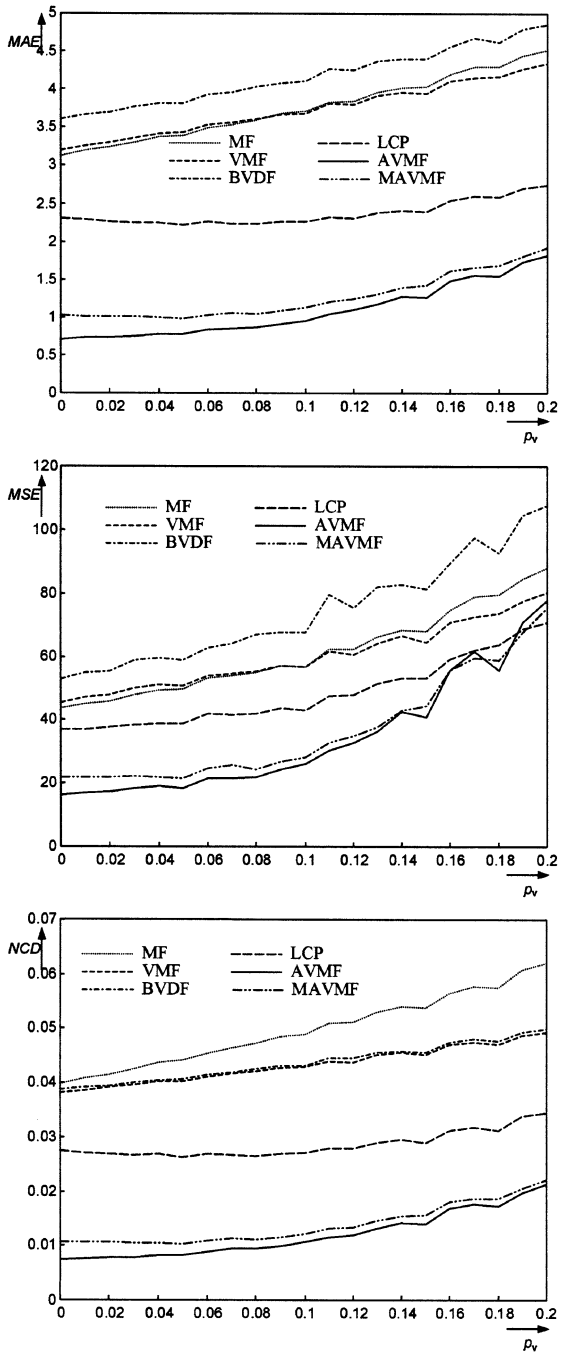

(a)

Figure 11. Performance of the methods expressed through MAE, MSE and NCD criteria in the dependence on the degree of the impulsive noise corruption $p_{\mathbf{V}}$: (a) test image Lena, (b) test image peppers.

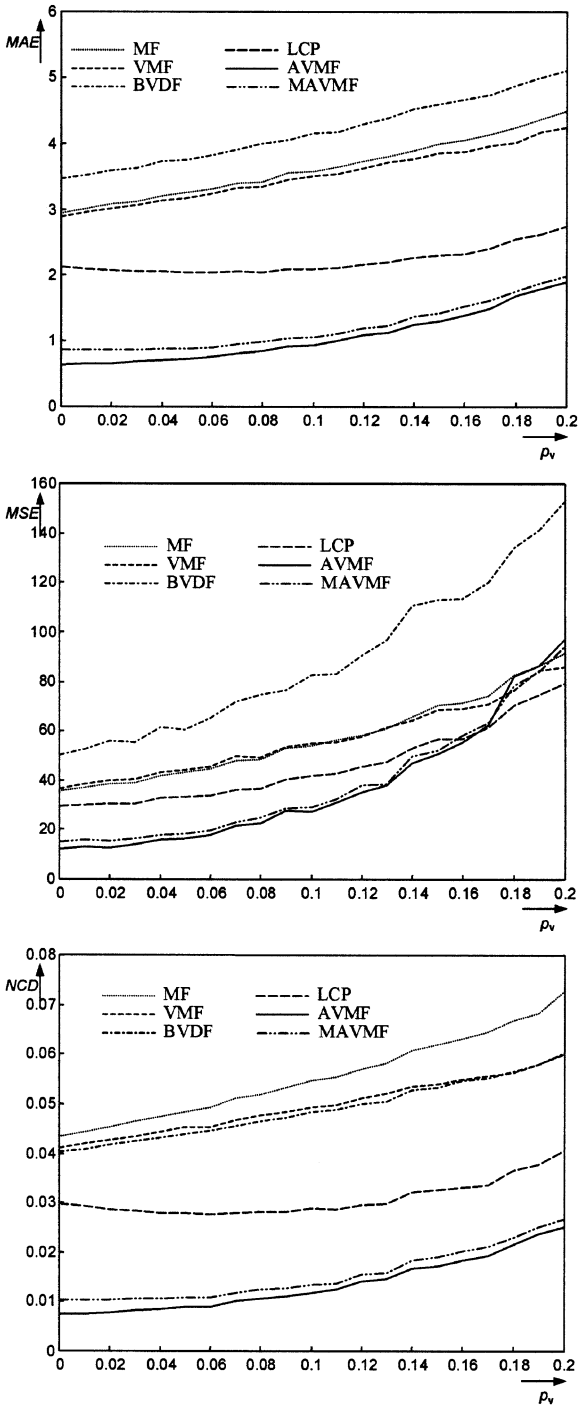

(b)

Figure 11. (Continued.)

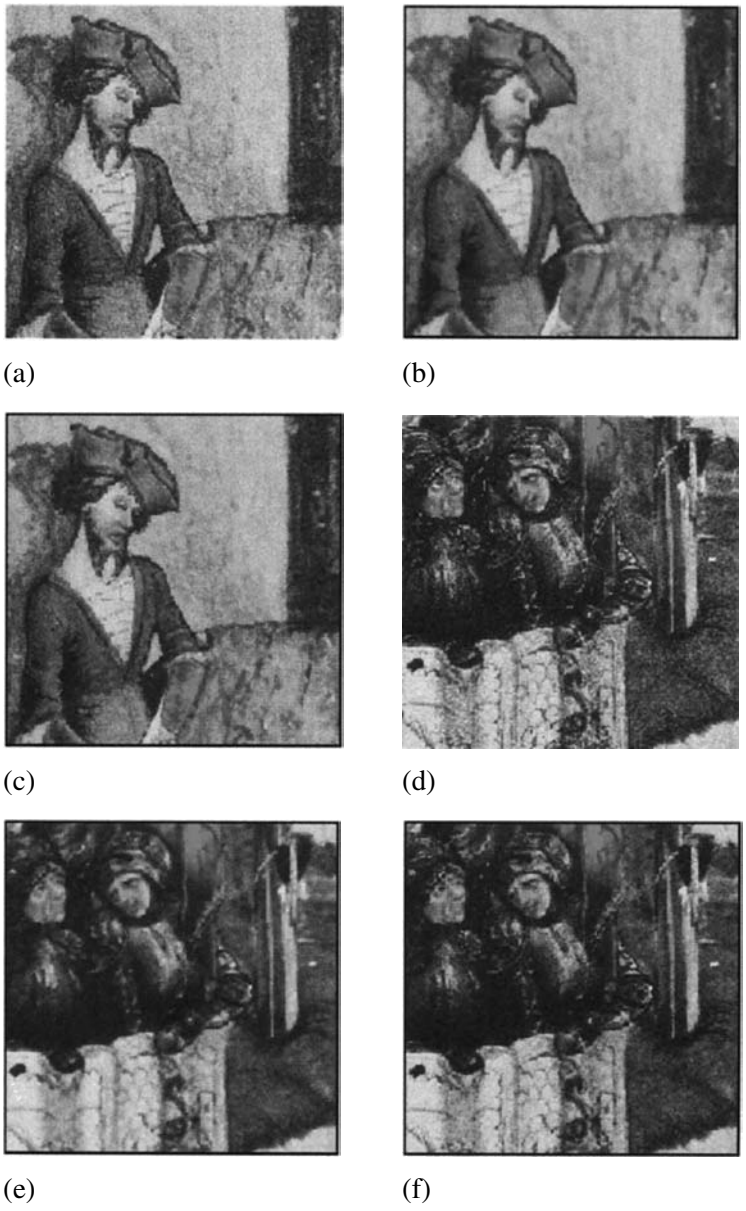

Figure 12. Real images represented by digitized images of fine arts: (a), (d) original images; (b), (e) images enhanced using the VMF scheme; (c), (f) images enhanced using the proposed AVMF scheme.

of the aggregated distances L_i related to each input $\mathbf{x}_i$, for $i = 1, 2, \ldots, N$, which are always required in all above-listed schemes. This comparison suggests that: (i) the computational complexity of both proposed adaptive solutions is signifi-

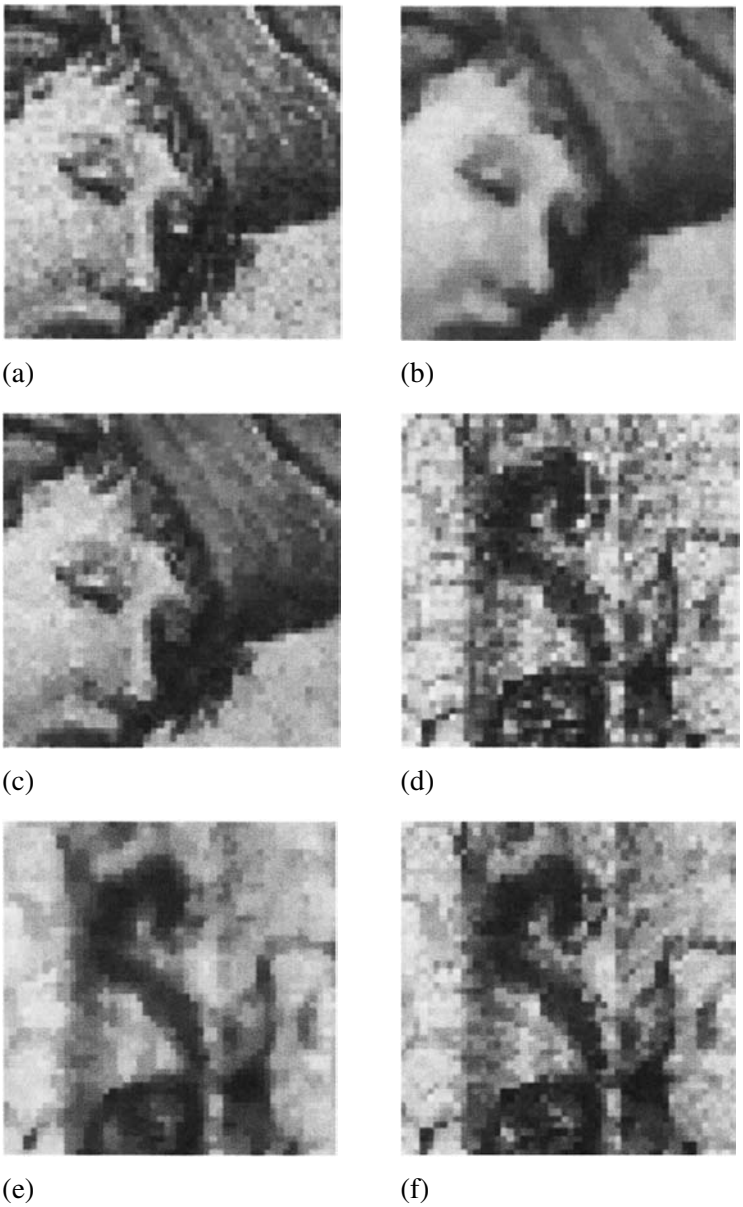

Figure 13. Zoomed parts of digitized fine arts and achieved results related to Figure 12: (a), (d) original images; (b), (e) images enhanced using the VMF scheme; (c), (f) images enhanced using the proposed AVMF scheme.

cantly lower than that of the SCWVDF scheme, and (ii) the proposed solutions and the VMF scheme are the most computationally efficient vector filters.

Finally, the efficiency of the zooming schemes is measured, in terms of the execution time, using a conventional PC equipped with a commonly used operating

Table IX. Number of elementary operations for a complete processing cycle corresponding to a 3×3 supporting window. The calculations for the switching schemes are provided for both non-smoothing (identity) and smoothing processing modes.

Filter/Operation	ADDs	MULTs	DIVs	SQRTs	COMPs	ARCCOSs
VMF	186	63	–	21	8	–
BVDF	375	210	21	21	8	21
DDF	540	282	21	42	8	21
SCWVDF (identity)	1143	684	66	69	25	66
SCWVDF (smoothing)	1518	894	87	90	33	87
Proposed AVMF (identity)	187	64	1	21	9	–
Proposed AVMF (smoothing)	187	64	1	21	9	–
Proposed MAVMF (identity)	78	28	4	9	1	–
Proposed MAVMF (smoothing)	264	91	4	30	9	–

system and a standard programming environment. When implemented in software, the execution of the proposed zooming tool on a PC with an Intel Pentium IV 2.40 GHz CPU, 512 MB RAM, Windows XP operating system and MS Visual C^{++} 5.0 programming environment, took (on average) 0.602 and 0.473 s per 256×256 color image with $p_{\mathbf{v}} = 0.10$ to be processed by AVMF and MAVMF schemes, respectively. The use of the VMF, BVDF, DDF and SCWVDF took 0.594, 1.672, 2.361, and 6.350 s, respectively. The recorded values suggest that the proposed adaptive filters constitute an efficient color image processing solution, which can be used in practical applications with the real-time processing constraints.

7. Conclusion

In this paper, a new multichannel approach viewed as the VMF adaptive modification for impulsive noise removal was proposed. The analysis performed as well as the results presented in the paper indicate that the proposed solutions exhibit an excellent balance between detail-preserving and noise-attenuating characteristics, while they are computationally efficient and can be relatively easily implemented either in hardware or software. Holding these properties, the new filters outperform well-known filtering schemes as well as their adaptive modifications. To boost further performance of the adaptive vector filters, future work will focus on the automatic setting of the adjusting parameter used in the proposed design.

References

1. Anderson, T. W.: *An Introduction to Multivariate Statistical Analysis*, 2nd edn, New York, Wiley, 1984.
2. Astola, J., Haavisto, P., and Neuvo, Y.: Vector median filters, *Proc. IEEE* **78** (1990), 678–689.

3. Astola, J. and Kuosmanen, P.: *Fundamentals of Nonlinear Digital Filtering*, CRC Press, Boca Raton, FL, 1997.
4. Barni, M., Bartolini, F., and Capellini, V: Image processing for virtual restoration of artworks, *IEEE Multimedia* (2000), 34–37.
5. Barni, M., Cappelini, V., and Mecocci, A.: Fast vector median filter based on Euclidean norm approximation, *IEEE Signal Processing Lett.* **1** (1994), 92–94.
6. Beghdadi, A. and Khellaf, K.: A noise-filtering method using a local information measure, *IEEE Trans. Image Processing* **6** (1997), 879–882.
7. Chapuis, R., Aufrere, R., and Chausse, F.: Accurate road following and reconstruction by computer vision, *IEEE Trans. Intelligent Transport. Systems* **3** (2002), 261–270.
8. Chen, T. and Wu, H. R.: Adaptive impulse detection using center-weighted median filters, *IEEE Signal Processing Lett.* **8** (2001), 1–3.
9. Eng, H. L. and Ma, K. K.: Noise adaptive soft-switching median filter, *IEEE Trans. Image Processing* **10** (2001), 242–251.
10. Forsyth, D. A. and Ponce, J.: *Computer Vision: A Moder Approach*, Prentice-Hall, Englewood Cliffs, NJ, 2002.
11. Gabbouj, M. and Cheickh, A.: Vector median–vector directional hybrid filter for color image restoration, in: *Proc. EUSIPCO-1996*, pp. 879–881.
12. Karakos, D. G. and Trahanias, P. E.: Generalized multichannel image-filtering structure, *IEEE Trans. Image Processing* **6** (1997), 1038–1045.
13. Kumar, R., Sawhney, R., Samarasekera, S., Hsu, S., Tao, H., Guo, Y., Hanna, K., Pope, A., Wildes, R., Hirvonen, D., Hansen, M., and Burt, P.: Aerial video surveillance and exploitation, *Proc. IEEE* **89** (2001), 1518–1539.
14. Lee, J. S.: Digital image smoothing and the sigma filter, *Computer Vision Graphics Image Processing* **24** (1983), 255–269.
15. Li, X., Lu, D., and Pan, Y.: Color restoration and image retrieval for Donhunag fresco preservation, *IEEE Multimedia* (2000), 38–42.
16. Lukac, R.: Adaptive color image filtering based on center-weighted vector directional filters, *Multidimensional Systems Signal Processing* **15** (2004), 169–196.
17. Lukac, R., Plataniotis, K. N., Smolka, B., and Venetsanopoulos, A. N.: Generalized selection weighted vector filters, *EURASIP J. Appl. Signal Processing*, Special Issue on Nonlinear Signal and Image Processing (2004), 1870–1885.
18. Lukac, R., Smolka, B., Martin, K., Plataniotis, K. N. and Venetsanopoulos, A. N.: Vector filtering for color imaging, *IEEE Signal Processing Magazine*, Special Issue on Color Image Processing **22** (2005), 74–86.
19. Lukac, R., Smolka, B., Plataniotis, K. N., and Venetsanopoulos, A. N.: Selection weighted vector directional filters, *Computer Vision Image Understanding*, Special Issue on Colour for Image Indexing and Retrieval **94** (2004), 140–167.
20. Lucat, L., Siohan, P., and Barba, D.: Adaptive and global optimization methods for weighted vector median filters, *Signal Processing Image Commun.* **17** (2002), 509–524.
21. Mardia, K. V., Kent, J. T., and Bibby, J. M.: *Multivariate Analysis*, Academic Press, New York, 1979.
22. Mustonen, S.: A measure for total variability in multivariate normal distribution, *Comput. Statistics Data Analysis* **23** (1997), 321–334.
23. Nosovsky, R. M.: Choice, similarity and the context theory of classification, *J. Experimental Psych. Learning Memory Cognition* **10** (1984), 104–114.
24. Pitas, I. and Tsakalides, P.: Multivariate ordering in color image filtering, *IEEE Trans. Circuits Systems Video Technol.* **1** (1991), 247–259.
25. Pitas, I. and Venetsanopoulos, A. N.: *Nonlinear Digital Filters, Principles and Applications*, Kluwer Academic Publishers, Dordrecht, 1990.

26. Pitas, I. and Venetsanopoulos, A. N.: Order statistics in digital image processing, *Proc. IEEE* **80** (1992), 1892–1919.
27. Plataniotis, K. N., Androutsos, D., and Venetsanopoulos, A. N.: Adaptive fuzzy systems for multichannel signal processing, *Proc. IEEE* **87** (1999), 1601–1622.
28. Plataniotis, K. N. and Venetsanopoulos, A. N.: *Color Image Processing and Applications*, Springer, Berlin, 2000.
29. Sharma, G. and Trussel, H. J.: Figures of merit for color scanners, *IEEE Trans. Image Processing* **6** (1997), 990–1001.
30. Tang, K., Astola, J., and Neuvo, Y.: Nonlinear multivariate image filtering techniques, *IEEE Trans. Image Processing* **4** (1995), 788–798.
31. Trahanias, P. E., Karakos, D., and Venetsanopoulos, A. M.: Directional processing of color images: Theory and experimental results, *IEEE Trans. Image Processing* **5** (1996), 868–881.
32. Viero, T., Oistamo, K., and Neuvo, Y.: Three-dimensional median related filters for color image sequence filtering, *IEEE Trans. Circuits Systems Video Technol.* **4** (1994), 129–142.
33. Zhang, S. and Karim, M. A.: A new impulse detector for switching median filters, *IEEE Signal Processing Lett.* **9** (2002), 360–363.
34. Zheng, J., Valavanis, K. P., and Gauch, J. M.: Noise removal from color images, *J. Intelligent Robotic Systems* **7** (1993), 257–285.
35. Lukac, R., Plataniotis, K. N., and Smolka, B.: Adaptive color image filter for application in virtual restoration of artworks, *IEEE Transactions on Multimedia*, submitted.